

Facial Manipulation Detection Based on the Color Distribution Analysis in Edge Region

Dong-Keon Kim
SungKyunKwan University
kdk1996@skku.edu

Donghee Kim
Hippo T&C
ym.dhkim@skku.edu

Kwangsue Kim
SungKyunKwan University
kim.kwangsue@skku.edu

Abstract

In this work, we present a generalized and robust facial manipulation detection method based on color distribution analysis of the vertical region of edge in a manipulated image. Most of the contemporary facial manipulation method involves pixel correction procedures for reducing awkwardness of pixel value differences along the facial boundary in a synthesized image. For this procedure, there are distinctive differences in the facial boundary between face manipulated image and unforged natural image. Also, in the forged image, there should be distinctive and unnatural features in the gap distribution between facial boundary and background edge region because it tends to damage the natural effect of lighting. We design the neural network for detecting face-manipulated image with these distinctive features in facial boundary and background edge. Our extensive experiments show that our method outperforms other existing face manipulation detection methods on detecting synthesized face image in various datasets regardless of whether it has participated in training.

1. Introduction

With rapid development of AI-based generative model [16, 29, 11], facial manipulation methods also improved in terms of generating realistic fake face image and changing one's face identity to others. As face synthesizing algorithms become more and more sophisticated, abuse cases and social issues derived from forged image have recently emerged. These realistically synthesized video for malicious purpose already becomes threat in terms of truth issue of public media, individual privacy [37], e.g., politician's fake news, celebrity pornography. For these reasons, detecting facial manipulated image effectively is crucial and important issue in computer vision field.

Existing works suggested their method with only focusing features that appear on the synthesized face image in datasets which generated by specific manipulation algo-

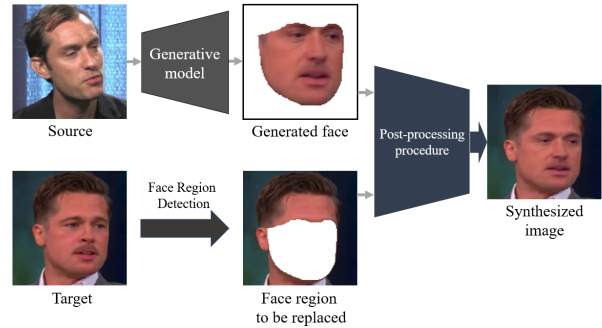


Figure 1. Summarized steps of face manipulation procedure. Generated image is created from source face image and generative model. For pasting generated image to target image realistically, post-processing is involved after image manipulation

rithms [23, 2, 38] or focusing on designing artificial neural network architectures [25, 1, 31] with referring whole image rather than paying attention to face manipulation procedure. Their own methods work well with specific datasets which they analyzed prior to design detection methods while they do not work well when it comes to classify synthesized video without prior information. Focusing on specific manipulation algorithms or referring whole image features is inefficient method when it comes to real-world scenario where we determine the authenticity of an arbitrary image without any prior information about the source data and manipulation procedures.

Most of face synthesizing algorithms nowadays commonly involve face boundary post-processing after face altering from one image to other image to reduce awkwardness of pixel distribution difference between original image and altered face image [19], as shown in Figure 1. Recent studies [18, 19, 33] pay attention to these shared procedures of face manipulation algorithms for detecting the synthesized image considering its generalization ability with other various datasets. Involved post-process procedure with face retouching application or generative model damages the

unique fingerprint in one image and makes the pixel distribution difference along face boundary area between post-processed manipulated image and unforged natural image.

Our work pays attention to extracting pixel value difference features along boundary area for detecting face manipulated image. With referring existing edge detector algorithms [27, 3], we gather set of vertical line of facial boundary and compute corresponding pixel difference along vertical lines. If a facial image is altered and gets post-processing procedure to smooth the facial boundary, there will be little difference in pixel values nearby face while unforged natural image has relatively large difference in pixel values nearby face because the pixel on the facial boundary were not modified.

Additionally, we gather boundary pixel differences along perpendicular line of background boundary. To analyze the difference with the feature extracted from the face boundary, the pixel difference values in the direction vertical to the background boundary are obtained in a similar method to facial feature extraction procedure. The difference between the features of the extracted background boundary and the features of the face boundary will be significantly different between the unforged natural image and the face manipulated image.

For classifying gathered features with outstanding performance, we use one-dimensional convolutional neural network which is used for extracting distinctive features in sequential data [12] because the gathered features are computed as pixel difference data which are ordered according to perpendicular direction of boundary of face and background. Rather than developing a complex and heavy classification model, we developed our own model that is lightweight and can classify with very good performance through the features we have extracted. We show our method with suggested classification model outperforms other existing manipulation detection in terms of model training stability and universality to other various datasets.

The contribution of this paper to the field of face manipulation detection is its outstanding performance and generalization regardless of dataset and generation algorithms. Our proposed method uses the pixel difference values as features and additionally uses information about the background of the image, so it does not bias toward specific source data or specific generation algorithms and performs with remarkably high detection accuracy regardless of face manipulation datasets.

2. Related Work

In this section, we will briefly introduce several previous image manipulation detection technologies from early studies of image forgery detection to the latest works which are related to our proposed method.

AI-generated image classification. In the beginning of re-

search about detecting AI-generated image, existing studies [39, 22, 24, 17] show that there is a difference in color distribution between the real image and entirely-created fake image made by AI-based generative model. There is a limitation of generative model that the image totally created leaves their own artificial imprints. AI-based generative model cannot perfectly reproduce original fingerprints of authentic natural image which made by intrinsic properties of hardware such as surface of camera lens and the direction of the light entering the camera. However, the problem of detecting manipulated images in which only the face region is altered must be approached slightly differently from the studies of determining authenticity of entirely generated images.

AI-Based Face Manipulation Detection. With rapidly progressed generative models and synthesizing techniques, there have been a lot of malicious usage such as realistically synthesizing one's face to other's body. For arising threats of these image forgery in terms of privacy and trust issues, there have been many studies [8, 21, 28] to detect face manipulated images. For instance, Matern et al. [23] present detection method based on visual artifacts, especially eyes and noses. Yang et al. [38] suggested a method of detecting face manipulation images through the inconsistency of the head pose. While these works pay attention to figure out some awkwardness features of synthesized image, recent works [25, 1, 31, 40], focus on detecting with well-designed state-of-the-arts artificial neural networks, such as recurrent neural network and capsule network.

All of these proposed works mainly focused on features appearing in synthesized image or designing the model architecture with synthesized image itself in specific datasets. Their works demonstrated only specific algorithms with limited source datasets while verifying with extensive experiment including real-world scenario for detecting unseen data with no prior information has failed.

Generalized Face Manipulation Detection. As the need for a methodology that can be better applied to real situations is increasing, the latest studies [4, 8] begin to focus on the characteristics that appear in the face image synthesis process rather than to the synthesized image result. Especially, Li et al. [19] pay attention to common procedure of face manipulation which include post-processing with boundary smoothing. Face X-ray [18], which is most recent work of generalized detection method focus on common blending procedure in various face manipulation algorithms and shows their generalization ability with unseen datasets for real-world scenario. Their work perform well with FaceForensics++ dataset which has several sub-datasets of different manipulation types with sharing source data, while experiences performance drop with totally different datasets. Our study further derive higher performance with more generality by extracting not only facial features,

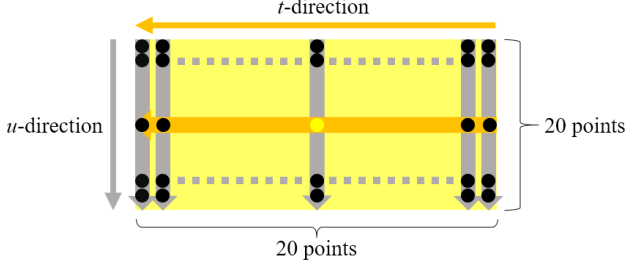


Figure 2. Brief illustration of edge window. Each point is spaced equally above the line segments. Center point in window implies mid-point $M_{i,i+1}$ of 2 neighboring landmark points, L_i and L_{i+1}

but also extracting innate fingerprints of background edges and comparing them with facial features.

3. Methods

In this section, we will explain the motivation of our methods, brief reason of gathering boundary pixel features, and detailed process of boundary feature extraction.

Motivation from Edge Detector Algorithm. We focus on existing edge detector algorithms for defining boundary. The edge detected by edge detector is the boundary point where the change of intensity is large based on the gray-scaled image [14]. Canny edge detector [3] which is the most used edge detector nowadays preferentially compute 1st order derivatives in the X and Y directions in given image by convolution with Sobel mask [32] before detecting edges in image. The gradient G in which the pixel value changes rapidly can be obtained with gathered 1st derivate values in X and Y directions. Gradient G implies the perpendicular direction of the boundary appearing in the image. We focused on the process of edge detector finding the boundary in an image through gradient. Since the distribution of pixel values of the face part in the image and the distribution of pixel values of the non-face parts are different, the pixel value will sharply change in a direction perpendicular to the boundary of the face.

Artificial Imprints Harming Natural Fingerprints. Early research in image forensic [10] mention that unforged natural image has a unique fingerprint generated in the procedure of image processing and hardware characteristics such as camera lens. However, recent studies [39, 22] show that forged images created by the generative models such as GAN has unique imprints from synthesizing procedure. Regardless of generative model types, the face replacing process and the post-processing process to reduce the difference in pixel values between the source image and the target image damage the natural image fingerprints across the facial boundary. For this reason, it is obvious that there is a difference between the synthesized facial boundary and the unforged natural image in terms of pixel values distribu-

tion. In addition, we emphasize the difference between the unmanipulated image and the forged image by contrasting the difference between the original fingerprint appearing on the background which is not involved in the facial synthesis process and the fingerprint on the face. Taking all of these into account, we can detect face manipulated image based on information of entire image and facial area in terms of boundary pixel feature.

Two-way feature extraction. We suggest two-way feature extraction method for detailed information in terms of two aspects, shared post-process procedure of face manipulation technology and boundary characteristics in whole image. One is facial boundary feature extraction which reflects pixel-level distributions by post-process procedure while the other is background boundary feature extraction which contains pixel-level distribution along boundary in unforged region of image.

3.1. Facial Boundary Feature Extraction

With a frame image I extracted from the video, we detect face area in image with frontal face detector in dlib [13]. It is assumed that only single face is appeared in the video. Then we extract 68 feature points of the detected face with 68 face landmark shape predictor in dlib. Among those detected landmarks, 17 points representing the outer boundary of the face are selected. These chosen landmark points are used to define the facial boundary in image. The line segment $P_{i,i+1}$ perpendicular to the facial boundary line is defined by vertical direction and midpoint of two neighboring landmark points L_i and L_{i+1} in facial boundary points.

Note that perpendicular line segment $P_{i,i+1}$ is parametric equation with parameter t which consists of 20 integer parameter with range -10 to 9, from inside of face to outside of face. There are 16 perpendicular line segments which made from 17 face landmark points representing facial boundary. Each $P_{i,i+1}$ have 20 corresponding coordinate information along vertical direction of boundary line at equal intervals.

To better reflect the perpendicular line segment in a specific area of the face, we tuned line segment size with scale-factor, which is inversely proportional to the facial area. By tuning with the scale-factor, the perpendicular line segment $P_{i,i+1}$ pass through a certain range of the facial boundary regardless of face size in image.

For making window-shaped coordinate features, set of horizontal line segments $V_{i,i+1}$ which are parallel to facial boundary line and go through the t -th point of gathered line segment $P_{i,i+1}$ is generated. Horizontal line segments are also represented by parametric equation with parameter u which has 20 integer parameters with range -10 to 9. Window-shaped 20×20 corresponding coordinates are specified by set of 20 horizontal lines. Figure 2 illustrates example of extracted edge window. We will call these 400

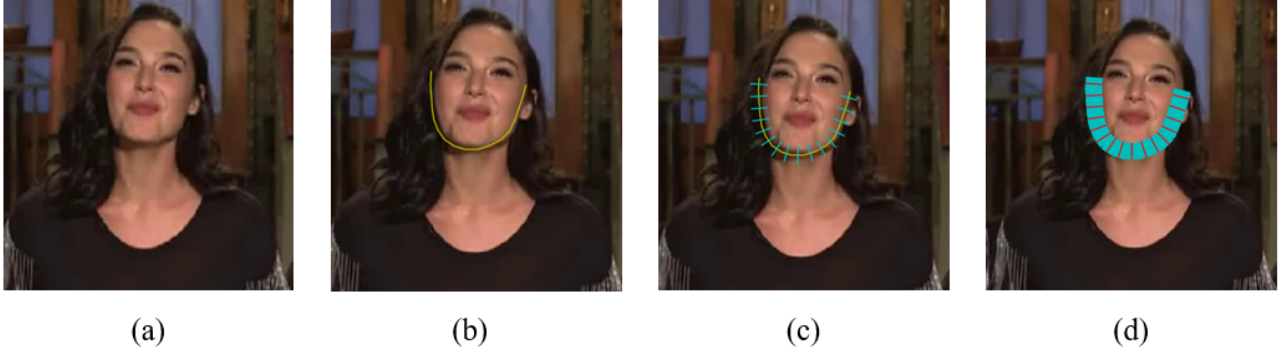


Figure 3. Facial boundary window generation pipeline. (a) Capture image I from video. (b) Get a facial boundary line with face landmark points detected from (a). (c) Make perpendicular line segment $P_{i,i+1}$ with neighboring landmark points. (d) Create set of horizontal lines $V_{i,i+1}$ perpendicular to line segment $P_{i,i+1}$ at equal intervals.

coordinate features to edge window W_i , which is set of horizontal lines $V_{i,i+1}$ with two parameter t and u . A total of 16 windows are created per face image with 17 facial boundary landmarks. Summarized pipeline of generating windows from one facial image is shown in Figure 3.

To find out how the corresponding RGB pixel values in edge window W_i change from the inside to the outside of the face, we compute the absolute difference of RGB pixel values according to the parameter t . Then we average pixel difference values in 20 horizontal lines for statistical difference in boundary region. These extracted $16 \times 19 \times 3$ color difference features are facial boundary features, 16 refers the number of edge windows W in one facial image, 19 indicates the differentiated feature along parameter t and 3 stands for RGB.

3.2. Background Boundary Feature Extraction

Prior to extracting the features of background edge points, we make a background edge image E_I from frame image I . For removing noise of background and extract prominent boundary parts, we blur the image I with Gaussian filter. Then rough edge image E'_I including edge points on face is generated with Canny edge detector.

Facial edge points in E'_I must be excluded for extract nature fingerprint of background edges. For removing facial edge points, we considered convex image C_I that covers face contour. C_I is binary image that has same size of original image I with inner points of convex are 0 and outer points of convex are 1. We would like to ensure that the edges appearing on the face were excluded. Big-face convex image C'_I is created by blurring C_I with Gaussian Filter and round down each value in blurred C_I to 0 except the pixels with the values of 1. With element-wise multiplying C'_I and E'_I , we can get edge image E_I which excludes facial edge points. Brief pipeline of making edge image E_I is

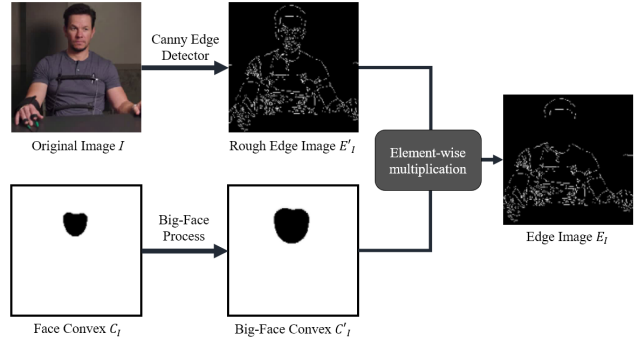


Figure 4. Background edge image generation procedure

shown at Figure 4.

For making background boundary feature from edge points in background edge image E_I , we randomly sampled 10% points of total edge points in E_I to get statistical information which appears along background edges. Using sampled edge points, background windows are extracted in a same way of facial boundary feature extraction, with L_i and L_{i+1} correspond to two nearest points of one sampled point. Summarized background edge windows generating procedure is shown at 5.

While edge windows in facial boundary have specified direction, from inside of face to outside of face with perpendicular direction, the direction of parameter t in background edge windows from background edge image cannot be specified except that they have vertical direction of boundary lines. For this reason, we fold the background boundary feature and unfold symmetrically with the basis on $T = 10$ for removing directional information in edge window, e.g., all feature values in $T = 1$ and $T = 19$ are averaged by axis and modified to averaged values. Final shape of mirrored background boundary color difference features

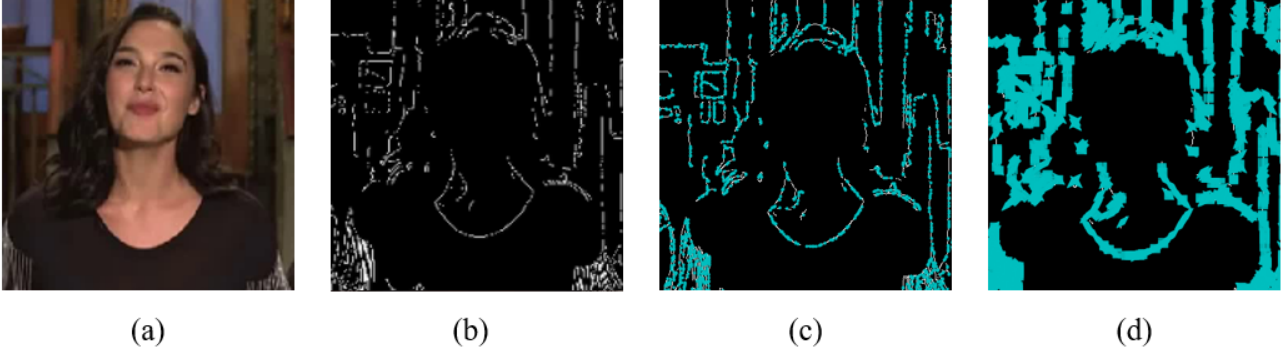


Figure 5. Background boundary feature extraction pipeline. (a) Capture image I from video. (b) Make a background edge image without facial boundary E_I . (c) Sample edge points in Edge Image from edge image E_I . (d) Make vertical lines and horizontal lines in the same way as the facial line segments were extracted.

has shape of $N \times 19 \times 3$. Note that N is the number of sampled edge points in background edge image E_F while 19 and 3 are same as mentioned in Section 3.1.

4. Analysis with Extracted Features

In this section, we briefly analyze how the features extracted from the image appear according to the authenticity of image prior to experimenting.

Datasets. We would like to analyze with various up-to-date face manipulation datasets with diverse generation algorithms for demonstrating our method’s generalization ability. We adopt several datasets: FaceForensics++ [30], Celeb-DF [20], DFD [6] and DFDC [7]. All of these datasets contains genuine video data and face manipulated video data from genuine ones with reduced awkwardness of pixel values. We randomly choose 750 genuine videos and 750 manipulated videos for FaceForensics++, DFD, and DFDC each. Exceptionally, since Celeb-DF dataset has less than 750 genuine video data, we choose 563 genuine video data and 750 manipulated video data in Celeb-DF dataset.

We plotted a graph to statistically analyze the change according to the parameter t value of the color features obtained by our method. Figure 6 shows difference value distributions along parameter t -direction from pre-processed facial features and background features in three datasets, Celeb-DF, FaceForensics++ and DFDC. Note that boundary edge points are at $t = 9$. We observe that there is a distribution difference between the facial features derived from the face manipulated image and the facial features extracted from the real image. There is significant difference in distribution points close to $t = 9$ point, which indicates the point along facial boundary line. Since a generated face image may have unusual pixel distribution in face boundary region because of post-processing methods to correct the difference in color values along the synthesized parts, the dif-

ference in color distribution is inevitable.

Also, the distribution seen in these three datasets have in common that the difference between facial features and background features is relatively larger for the unforged image than for the face manipulated image. This observation shows that reflecting the facial information and background information together could help solve the problem of generality.

5. Experiment

In this section, we introduce our experiment setups, implementation details and result of extensive experiment with aspect of overall performance, universality and comparison with other contemporary works to verify our methods.

For conclusive evaluation of detection performance, we mainly trained with Celeb-DF dataset, which is difficult for other papers to derive remarkable detection performance [36] and use FaceForensics++, DFD, DFDC datasets additionally. When testing, we cross-validate through all of these datasets to demonstrate universality of our method.

Additional preprocessing for experiment. We would like to get information of difference between the distribution indicated by the difference in color values at the edge region with aspect of face and background. We get difference value with following Equ. (1)

$$D_{I,n} = F_{I,n} - \hat{B}_I \quad (1)$$

Note that $F_{I,n}$, \hat{B}_I and $D_{I,n}$ indicate facial boundary feature in n th window, averaged background boundary feature, and difference between $F_{I,n}$ and \hat{B}_I each. Final features derived from background edge region is $D_{I,n}$ with a shape of $16 \times 19 \times 3$. Then we flatten the facial feature which extracted in Section 3.1 from shape $16 \times 19 \times 3$ to 304 linear feature with 3 RGB channels. Also, the background features which extracted from Section 3.2 are flattened in the

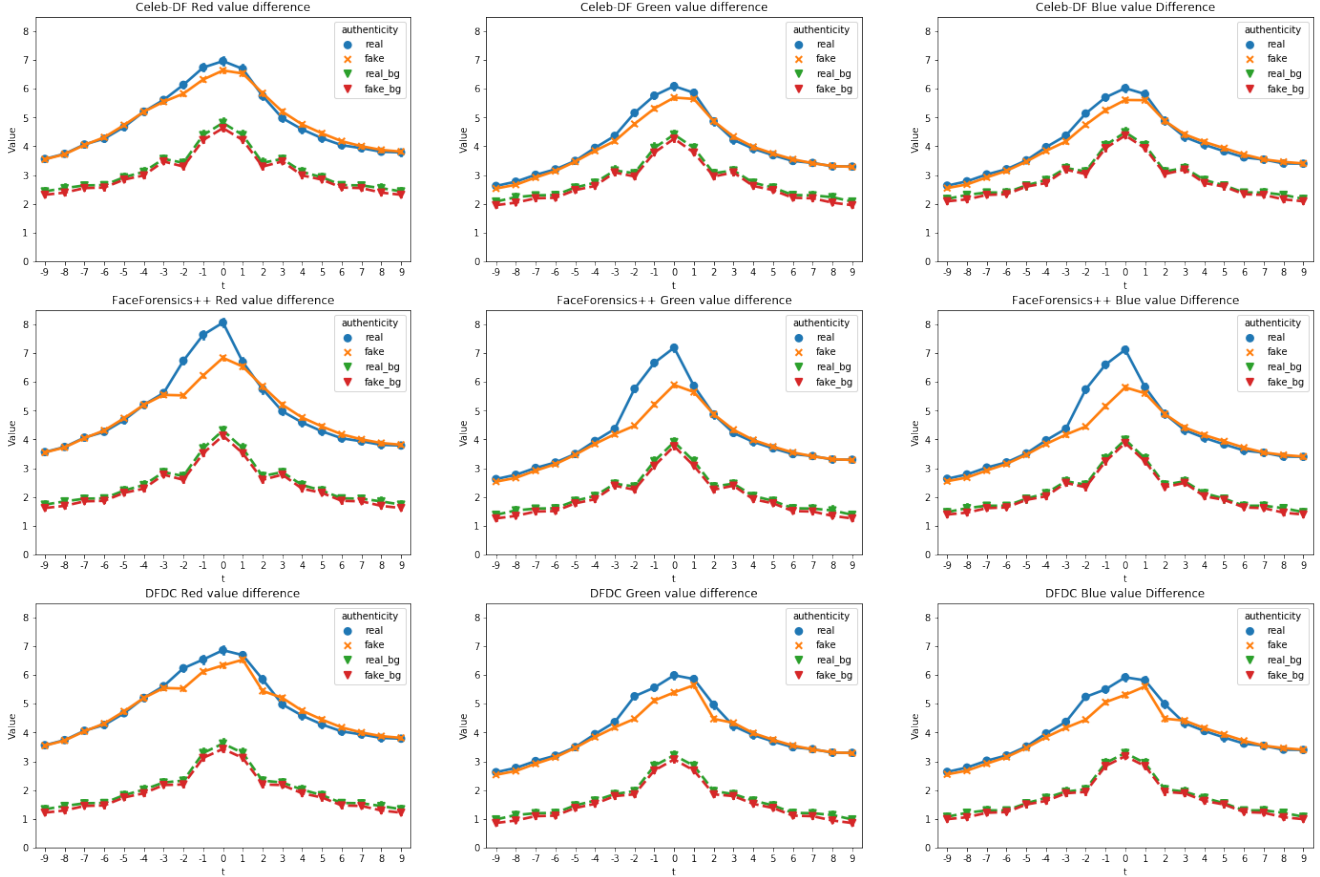


Figure 6. Color difference distribution of extracted features from 3 different datasets.

same way. The input shape of the preprocessed features for the classification model has a 6-channel 304 linear feature consisting of 3 channels of flatten face features and 3 channels of flatten background features.

Classification Model. To further highlight distinctive features between unforged image and face manipulated image, we adopt 1-dimensional convolutional neural networks (1D-CNN) which is widely used in the field of natural language processing for extracting features from sequential inputs [12] unlike other existing manipulation detection models [30, 7] using 2-dimensional convolutional neural networks (2D-CNN) to process image features, since the extracted color difference features are sequential data according to the parameter t . While advanced face manipulated image classification models are mainly designed to be complex and heavy for extracting significant information from whole images, we constructed a lightweight simple model to process our pre-processed distinctive color features. The number of total epoch is set to 1000 and the batch size is set to 20. The learning rate is set as 0.00075 using Adam [15] optimizer. Additionally we scheduled optimizer to multiply 0.5 to learning rate at every 200 epochs for decaying learn-

Performance (AUC)			
Study	FF++ / DFD	DFDC	Celeb-DF
Matern et al. [23]	78.0	66.2	55.1
Yang et al. [38]	47.3	55.9	54.6
Li et al. [19]	93.0	75.5	64.6
Zhou et al. [40]	70.1	61.4	53.8
Nguyen et al. [25]	96.6	53.3	57.5
Ours	99.8	97.9	95.2

Table 1. Performance result compared with recent works

ing rate. Cross-entropy function is used for loss function.

5.1. Detection Performance with Specific Dataset

We firstly experiment with one specific dataset for both training and testing. To evaluate our experiment results, several existing methods results [23, 38, 19, 40, 25] which are validated with all of four state-of-the-arts datasets (FaceForensics++, DFD, DFDC and Celeb-DF) cited from their original paper are shown with our results. Summarized performance compared with referred five manipulation detec-

Performance (AUC)					
		Test set			
Study	Training set	FF++	DFD	DFDC	Celeb-DF
Xception [30]	FF++	-	87.8	54.3	40.9
Face X-ray [18]	FF++ and BI	98.52	95.4	80.92	80.58
Ours	FF++	99.8	95.1	89.5	87.7

Table 2. Generalization ability comparison with Xception Network, Face X-ray and ours with several datasets. BI indicates generated additional dataset made by FaceForensics++ datasets with applying method of Face X-ray [18]

Cross-Validation Performance (AUC)				
Training set	Test set			
	FF++	DFD	DFDC	Celeb-DF
FF++	99.8	95.1	89.5	87.7
DFD	95.9	99.8	88.5	87.6
DFDC	98.5	93.0	97.9	88.3
Celeb-DF	99.8	99.5	97.1	95.2

Table 3. Cross-validation Performance result

Performance (AUC)		
Study	FF++/DF	Celeb-DF
FWA [19]	79.2	53.8
Face X-ray [18]	99.2	74.8
Ours	99.8	95.2

Table 4. Performance comparison with FWA and Face X-ray

Performance (AUC))		
Study	Test set	
	Face2Face	FaceSwap
Du et al. [8]	90.9	63.2
Nguyen et. al [26]	92.8	54.1
Riess et al. [4]	94.5	72.6
Ours	99.8	95.5

Table 5. Performance comparison with 3 other recent works training with Face2Face dataset.

tion methods in terms of AUC, which is area under the Receiver Operating Characteristic curve is in Table 1. We observe that our performance results outperform those of the other papers mentioned, especially in terms of verifying with Celeb-DF dataset (95.2%) which makes other advanced manipulation detection methods performance drastically dropped.

5.2. Cross-Validation with Various Datasets

We design cross-validation experiment for testing our approach with aspect of robustness to real-world scenarios. In this experiment, we train our model with one dataset and test with the other dataset for making scenarios that detect manipulated image with unseen dataset. Ta-

ble 3 shows cross-validation performance result of our approach in terms of AUC. We observed that cross-validating with Celeb-DF features trained model can obtain more generalized results compared with trained model with other datasets. These inconsistency by training sets may be occurred because the extracted feature from Celeb-DF dataset have relatively less distinctive difference between unforged image and manipulated image compared with other three datasets. We can see that a model trained with a dataset with a relatively less prominence features such as Celeb-DF performs well when verifying a dataset with more prominent features. Nevertheless, any experiment results with DFDC and Celeb-DF as test dataset outperforms any other referred face manipulation detection methods.

5.3. Comparison with Latest Works

For more precise evaluation with aspect of universality, we compared our performance result with latest works [30, 19, 18, 4, 8, 26] in terms of generalization ability. Table 4 shows the comparison of best performance with ours and Face X-ray [18] in terms of training with one sub-dataset in FaceForensics++ [30] and testing with other dataset. There are 4 sub-datasets in FaceForensics++ datasets, including DeepFake [5], Face2Face [35], FaceSwap [9], NeuralTextures [34]. We cite two compared results directly in [18], XceptionNet results from [30] and Face X-ray results. Table 2 summarizes AUC results compared with these existing contemporary works and ours. Although we cannot reproduce exactly same BI datasets which additionally generated from FaceForensics++ datasets with mentioned method in [18], we can see the our framework outperform other two approaches with aspects of best performance of AUC.

We also present the AUC of verifying with one dataset compared with Face Warping Artifacts [19] and Face X-ray [18] in Table 4. Our approach shows better results in both detection performance with specific dataset, and universality for various face synthesizing algorithms universality.

Lastly, we compare with other 3 recent works which suggest other approaches for universality. Each studies focus on learning innate representation in manipulated image [4, 8] and do detection and localization of synthesized feature simultaneously [26]. Table 5 shows the generalization ability results compared with referred 3 works [4, 8, 26]. We

observe that our approach can show better performance in terms of universality for different type of synthesizing algorithm. compared with other studies which don't approach with aspect of common manipulation procedure of synthesizing algorithms.

6. Conclusion

We present a face manipulation detection methods with leveraging facial boundary features which corresponding to color features modified by common boundary post-processing of generation procedures. In addition to referring facial features, background features corresponding to unchanged characteristics containing image's innate fingerprints are used for detecting face synthesized image. We reveal the importance of utilizing both facial edge information and background edge information with outstanding detection performance better than other existing advanced face manipulation detection methods. Cross-validating with state-of-the-arts datasets demonstrate our approach not only remarkably performed with specific dataset but can also be fully applied in real-world situations.

References

- [1] Darius Afchar et al. "Mesonet: a compact facial video forgery detection network". In: *2018 IEEE International Workshop on Information Forensics and Security (WIFS)*. IEEE. 2018, pp. 1–7.
- [2] Shruti Agarwal et al. "Protecting World Leaders Against Deep Fakes." In: *CVPR Workshops*. 2019, pp. 38–45.
- [3] John Canny. "A computational approach to edge detection". In: *IEEE Transactions on pattern analysis and machine intelligence* 6 (1986), pp. 679–698.
- [4] Davide Cozzolino et al. "Forensictransfer: Weakly-supervised domain adaptation for forgery detection". In: *arXiv preprint arXiv:1812.02510* (2018).
- [5] Deepfakes. *deepfakes/faceswap*. URL: <http://www.github.com/deepfakes/faceswap>.
- [6] DFD. *Contributing Data to Deepfake Detection Research*. Sept. 2019. URL: <https://ai.googleblog.com/2019/09/contributing-data-to-deepfake-detection.html>.
- [7] Brian Dolhansky et al. *The Deepfake Detection Challenge (DFDC) Preview Dataset*. 2019. arXiv: 1910.08854 [cs.CV].
- [8] Mengnan Du et al. "Towards generalizable forgery detection with locality-aware autoencoder". In: *arXiv preprint arXiv:1909.05999* (2019).
- [9] Faceswap. *MarekKowalski/FaceSwap*. URL: <http://www.github.com/MarekKowalski/FaceSwap>.
- [10] Hany Farid. "A survey of image forgery detection". In: *IEEE Signal Processing Magazine* 2.26 (2009), pp. 16–25.
- [11] Ian Goodfellow et al. "Generative Adversarial Nets". In: *Advances in Neural Information Processing Systems*. Ed. by Z. Ghahramani et al. Vol. 27. Curran Associates, Inc., 2014, pp. 2672–2680. URL: <https://proceedings.neurips.cc/paper/2014/file/5ca3e9b122f61f8f06494c97b1afccf3-Paper.pdf>.
- [12] Yoon Kim. "Convolutional neural networks for sentence classification". In: *arXiv preprint arXiv:1408.5882* (2014).
- [13] Davis E King. "Dlib-ml: A machine learning toolkit". In: *The Journal of Machine Learning Research* 10 (2009), pp. 1755–1758.
- [14] Paul H King. "Digital image processing and analysis: Human and computer applications with cvip-tools, (umbaugh, s.; 2011)[book reviews]". In: *IEEE Pulse* 3.4 (2012), pp. 84–85.
- [15] Diederik P Kingma and Jimmy Ba. "Adam: A method for stochastic optimization". In: *arXiv preprint arXiv:1412.6980* (2014).
- [16] Diederik P Kingma and Max Welling. *Auto-Encoding Variational Bayes*. 2014. arXiv: 1312.6114 [stat.ML].
- [17] Haodong Li et al. "Detection of deep network generated images using disparities in color components". In: *arXiv preprint arXiv:1808.07276* (2018).
- [18] L. Li et al. "Face X-Ray for More General Face Forgery Detection". In: *2020 IEEE/CVF Conference on Computer Vision and Pattern Recognition (CVPR)*. 2020, pp. 5000–5009. DOI: 10.1109/CVPR42600.2020.00505.
- [19] Yuezun Li and Siwei Lyu. "Exposing deepfake videos by detecting face warping artifacts". In: *arXiv preprint arXiv:1811.00656* (2018).
- [20] Yuezun Li et al. *Celeb-DF: A Large-scale Challenging Dataset for DeepFake Forensics*. 2020. arXiv: 1909.12962 [cs.CR].
- [21] Francesco Marra et al. "Detection of gan-generated fake images over social networks". In: *2018 IEEE Conference on Multimedia Information Processing and Retrieval (MIPR)*. IEEE. 2018, pp. 384–389.

- [22] Francesco Marra et al. “Do gans leave artificial fingerprints?” In: *2019 IEEE Conference on Multimedia Information Processing and Retrieval (MIPR)*. IEEE. 2019, pp. 506–511.
- [23] Falko Matern, Christian Riess, and Marc Stamminger. “Exploiting visual artifacts to expose deep-fakes and face manipulations”. In: *2019 IEEE Winter Applications of Computer Vision Workshops (WACVW)*. IEEE. 2019, pp. 83–92.
- [24] Scott McCloskey and Michael Albright. “Detecting GAN-generated imagery using saturation cues”. In: *2019 IEEE International Conference on Image Processing (ICIP)*. IEEE. 2019, pp. 4584–4588.
- [25] H. H. Nguyen, J. Yamagishi, and I. Echizen. “Capsule-forensics: Using Capsule Networks to Detect Forged Images and Videos”. In: *ICASSP 2019 - 2019 IEEE International Conference on Acoustics, Speech and Signal Processing (ICASSP)*. 2019, pp. 2307–2311. DOI: [10.1109/ICASSP.2019.8682602](https://doi.org/10.1109/ICASSP.2019.8682602).
- [26] Huy H Nguyen et al. “Multi-task learning for detecting and segmenting manipulated facial images and videos”. In: *arXiv preprint arXiv:1906.06876* (2019).
- [27] Judith MS Prewitt. “Object enhancement and extraction”. In: *Picture processing and Psychopictorics* 10.1 (1970), pp. 15–19.
- [28] Weize Quan et al. “Distinguishing between natural and computer-generated images using convolutional neural networks”. In: *IEEE Transactions on Information Forensics and Security* 13.11 (2018), pp. 2772–2787.
- [29] Danilo Jimenez Rezende, Shakir Mohamed, and Daan Wierstra. “Stochastic Backpropagation and Approximate Inference in Deep Generative Models”. In: ed. by Eric P. Xing and Tony Jebara. Vol. 32. *Proceedings of Machine Learning Research* 2. Beijing, China: PMLR, 22–24 Jun 2014, pp. 1278–1286. URL: <http://proceedings.mlr.press/v32/rezende14.html>.
- [30] Andreas Rossler et al. “FaceForensics++: Learning to Detect Manipulated Facial Images”. In: *Proceedings of the IEEE/CVF International Conference on Computer Vision (ICCV)*. Oct. 2019.
- [31] Ekraam Sabir et al. “Recurrent convolutional strategies for face manipulation detection in videos”. In: *Interfaces (GUI)* 3.1 (2019).
- [32] Irwin Sobel and Gary Feldman. “A 3x3 isotropic gradient operator for image processing”. In: *a talk at the Stanford Artificial Project in* (1968), pp. 271–272.
- [33] Joel Stehouwer et al. “On the detection of digital face manipulation”. In: *arXiv preprint arXiv:1910.01717* (2019).
- [34] Justus Thies, Michael Zollhöfer, and Matthias Nießner. “Deferred Neural Rendering: Image Synthesis Using Neural Textures”. In: *ACM Trans. Graph.* 38.4 (July 2019). ISSN: 0730-0301. DOI: [10.1145/3306346.3323035](https://doi.org/10.1145/3306346.3323035). URL: <https://doi.org/10.1145/3306346.3323035>.
- [35] Justus Thies et al. “Face2Face: Real-Time Face Capture and Reenactment of RGB Videos”. In: *Commun. ACM* 62.1 (Dec. 2018), pp. 96–104. ISSN: 0001-0782. DOI: [10.1145/3292039](https://doi.org/10.1145/3292039). URL: <https://doi.org/10.1145/3292039>.
- [36] Ruben Tolosana et al. “Deepfakes and beyond: A survey of face manipulation and fake detection”. In: *arXiv preprint arXiv:2001.00179* (2020).
- [37] Cristian Vaccari and Andrew Chadwick. “Deepfakes and disinformation: exploring the impact of synthetic political video on deception, uncertainty, and trust in news”. In: *Social Media+ Society* 6.1 (2020), p. 2056305120903408.
- [38] Xin Yang, Yuezun Li, and Siwei Lyu. “Exposing deep fakes using inconsistent head poses”. In: *ICASSP 2019-2019 IEEE International Conference on Acoustics, Speech and Signal Processing (ICASSP)*. IEEE. 2019, pp. 8261–8265.
- [39] Ning Yu, Larry S Davis, and Mario Fritz. “Attributing fake images to gans: Learning and analyzing gan fingerprints”. In: *Proceedings of the IEEE International Conference on Computer Vision*. 2019, pp. 7556–7566.
- [40] Peng Zhou et al. “Two-stream neural networks for tampered face detection”. In: *2017 IEEE Conference on Computer Vision and Pattern Recognition Workshops (CVPRW)*. IEEE. 2017, pp. 1831–1839.